Design Sensitivity Analysis and Optimization for Nonlinear Buckling of Finite-Dimensional Elastic Conservative Structures[1]

M. Ohsaki

Department of Architecture and Architectural Engineering,
Kyoto University Kyotodaigaku-Katsura, Nishikyo, Kyoto 615-8540, Japan
E-mail: ohsaki@archi.kyoto-u.ac.jp

Abstract

The purpose of this review paper is to summarize the existing methods of design sensitivity analysis and optimization of elastic conservative finite dimensional systems with respect to nonlinear buckling behavior. Difficulties related to geometrical nonlinear singular behaviors are discussed in detail. Characteristics of optimized structures are demonstrated in reference to snapthrough behavior, hill-top branching, and degenerate critical points. A new optimization result of a flexible truss that fully utilizes the snapthrough behavior is also presented.

Keywords Optimum design; Geometrical Nonlinearity; Stability; Sensitivity analysis

1 Introduction

In the early stage of optimum design under buckling constraints, optimal shapes of columns were investigated by analytical approaches. Prager and Taylor (50) derived optimality conditions for columns under linear buckling constraints. Since then, numerous number of works have been published on sensitivity analysis and optimization of column-type structures under linear buckling constraints, where difficulties due to discontinuity of sensitivity coefficients related to multiple eigenvalues have been extensively discussed. Optimization methods of columns under linear buckling constraints are not included in this review article, because they can be found in the literature (45; 14; 57).

Optimization of finite-dimensional structures against buckling started in 1970's. Linear buckling formulation was first used neglecting prebuckling deformation. Khot *et al.* (24) presented an optimality criteria approach for trusses and frames. They applied their method to a shallow truss, although it is clear that prebuckling deformation should be incorporated for those structures. In 1980's, more practical problems were studied incorporating constraints on displacements and stresses as well as linear buckling load factor (33). Difficulties due to multiple eigenvalues also exist for finite dimensional structures. Recently, it was shown that the optimum design with

[1]This paper has appeared in: Comp. Meth. Appl. Mech. Engng., Vol. 194, pp. 3331–3358, 2005.

multiple linear buckling load factors can be found by successively solving SemiDefinite Programming (SDP) (22; 29) without any difficulty by using an interior point method.

Small trusses exhibiting limit point instability were studied in the early stage of optimization of geometrically nonlinear finite dimensional structures (49). The maximum total potential energy was also used as the performance measure (23), although it is not clear if maximization of the total potential energy is equivalent to that of the limit point load factor. Kamat and Ruangsingha (21) presented a mathematical programming approach for maximizing limit point loads.

In 1990's, numerical approaches were presented for optimum designs of moderately large geometrically nonlinear structures. Optimality criteria approaches were mainly used for maximizing the limit point load factor (55; 32). Although iterative approaches that are similar to the fully stressed design are simple to implement, the optimality of the solutions derived by those methods is not theoretically clear. Ohsaki and Nakamura (42) presented a method based on parametric programming approach.

For building frames, optimization methods were developed independently from general finite dimensional structures, because they have unique situation such as brace buckling and interaction of local and global buckling modes (27). Numerical methods utilizing the characteristics of building frames were developed by Hall *et al.* (13) and Bažant and Xiang (3). Hjelmstad and Pezeshk (15) presented an optimality criteria approach for buckling and displacement constraints under lateral loads.

In this paper, methods of sensitivity analysis of geometrically nonlinear buckling loads and formulations of optimization problems are reviewed. Note that problems relating to linear buckling are out of scope of this paper. In the following, *geometrical nonlinearity* means effect of large deformation, where the strains are restricted in a small range. Historical backgrounds as well as scopes for future research are included. Only conservative systems subjected to quasi-static proportional loads are considered. Non-conservative systems, dynamic problems, control problems, and path-dependent problems are beyond scope of this review. Although we concentrate on finite dimensional systems, the methods and problem formulations presented in this paper are valid also for continuum discretized by a finite element approach.

In Section 2, the basic equations and classification of critical points are briefly presented. In Section 3, possible formulations of optimization problems and difficulties for obtaining optimal solutions are discussed in relation to snapthrough behavior. The existing methods of sensitivity analysis of geometrically nonlinear responses and critical load factors are reviewed in Section 4. The difficulties due to hill-top branching and degenerate critical point are presented in Section 5. In Section 6, existing studies on imperfection sensitivity of optimized structures are shown. Finally in Section 7, a new result is presented for a flexible truss to generate large deformation efficiently by incorporating snapthrough behavior.

2 Geometrically nonlinear analysis.

Consider a finite dimensional elastic structure subjected to quasi-static proportional loads $\mathbf{P} = \Lambda\mathbf{p}$, where Λ is the load factor and $\mathbf{p}$ is the specified vector of load pattern. Let $\mathbf{A}$ denote the vector of design variables such as stiffnesses of elements and locations of nodes. Note that $\mathbf{p}$ is also a function of $\mathbf{A}$ for the case, e.g. self-weight is considered. The vector of nodal displacements is denoted by $\mathbf{U}(\Lambda, \mathbf{A}) = \{U_i(\Lambda, \mathbf{A})\}$ which is a function of Λ and $\mathbf{A}$. In the following, a subscript is used for indicating an element of a vector.

Equilibrium equations are given as

$$\mathbf{F}(\mathbf{U}(\Lambda, \mathbf{A}), \mathbf{A}) = \Lambda\mathbf{p}(\mathbf{A}) \tag{1}$$

where $\mathbf{F}$ is the vector of equivalent nodal loads defined as a nonlinear function of $\mathbf{U}(\Lambda, \mathbf{A})$ and $\mathbf{A}$. In the following, the arguments $\mathbf{U}$, Λ and $\mathbf{A}$ are written explicitly only when defining a new variable or dependence on these variables should be clearly stated. The curve in the $\mathbf{U} - \Lambda$ space formed by the points that satisfy the equilibrium equation (1) is called *equilibrium path* that is traced by an incremental and/or iterative approach. The equilibrium path that originate from the undeformed initial state is called fundamental equilibrium path. Green's strain and the second Piola-Kirchhoff stress are usually used for defining geometrically nonlinear strain-displacement relation and the constitutive relation of the elastic material. In some cases, e.g. for a large and complex structure, it is not straightforward to construct analysis model and to trace the equilibrium path. However, the objective of this paper is to present optimization formulations and sensitivity analysis methods corresponding to nonlinear buckling. The details on geometrically nonlinear analysis may be consulted to, e.g. Refs. (8; 2).

Let $S(\mathbf{U}(\Lambda, \mathbf{A}), \mathbf{A})$ denote the total strain energy of the structure. For an elastic conservative system subjected to proportional nodal loads, $\mathbf{F}$ can be obtained from the stationary conditions of S as

$$F_i = \frac{\partial S}{\partial U_i}, \quad (i = 1, 2, \ldots, n) \tag{2}$$

where n is the number of degrees of freedom. The total potential energy $\Pi(\mathbf{U}(\Lambda, \mathbf{A}), \Lambda, \mathbf{A})$ is defined as

$$\Pi(\mathbf{U}(\Lambda, \mathbf{A}), \Lambda, \mathbf{A}) = S(\mathbf{U}(\Lambda, \mathbf{A}), \mathbf{A}) - \Lambda\mathbf{U}(\Lambda, \mathbf{A})^\top\mathbf{p}(\mathbf{A}) \tag{3}$$

where $(\ )^\top$ indicates the transpose of a vector or a matrix. The equilibrium equation is written by the stationary condition of Π as

$$\begin{aligned} \frac{\partial \Pi}{\partial U_i} &= \frac{\partial S}{\partial U_i} - \Lambda p_i \\ &= F_i - \Lambda p_i \\ &= 0, \quad (i = 1, 2, \ldots, n) \end{aligned} \tag{4}$$

The tangent stiffness matrix $\mathbf{K}$ is defined as the Jacobian matrix of $\mathbf{F}$ or Hessian of Π with respect to $\mathbf{U}$; i.e. the (i,j)-component K_{ij} of $\mathbf{K}$ is obtained from

$$K_{ij} = \frac{\partial F_i}{\partial U_j} = \frac{\partial^2 \Pi}{\partial U_i \partial U_j}, \quad (i,j = 1,2,\ldots,n) \tag{5}$$

The detailed process and the computational difficulties for computing $\mathbf{K}$ are also out of scope of this paper.

Let λ_r and Φ_r denote the rth eigenvalue and eigenvector of $\mathbf{K}$; i.e.

$$\mathbf{K}\Phi_r = \lambda_r \Phi_r, \quad (r = 1,2,\ldots,n) \tag{6}$$

where Φ_r is normalized by

$$\Phi_r^\top \Phi_r = 1, \quad (r = 1,2,\ldots,n) \tag{7}$$

The critical load factor, or the nonlinear buckling load factor, Λ^{c} is defined as the value of Λ that satisfies $\lambda_1 = 0$, where λ_1 is the lowest eigenvalue of $\mathbf{K}$. Define β by

$$\beta = \sum_{i=1}^{n} p_i \Phi_{1i}^{\mathrm{c}} \tag{8}$$

where Φ_{1i}^{c} is the ith component of the lowest eigenvector at the critical point. The critical points are classified as

$$\begin{aligned} &\text{Limit point :} && \beta \neq 0 \\ &\text{Bifurcation point :} && \beta = 0 \end{aligned} \tag{9}$$

It can be seen from (8) and (9) that the buckling mode Φ_1 is orthogonal to the load vector for the bifurcation point. The details of the classification are not presented here, because only (9) should be clearly stated for discussing the differences between sensitivity analysis methods of limit point and bifurcation loads.

There are many numerical approaches for finding the critical points (66; 52; 10). The critical point can be pinpointed within arbitrary accuracy by iteratively solving the extended system formulated by (4) and (6) for $r = 1$, $\lambda_1 = 0$. Since the computation of critical points is beyond the scope of this review paper, it is assumed in the following that the critical points can be found within arbitrary good accuracy.

3 Formulation of optimum design problem and difficulties due to snapthrough behavior.

3.1 Illustrative example of a 2-bar truss

To illustrate the difficulties in optimization of geometrically nonlinear structures considering buckling behavior, three cases as listed in Table 1 are solved for a 2-bar truss

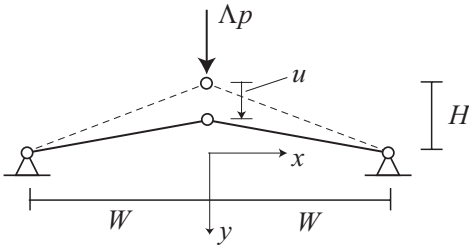

Fig. 1: A 2-bar truss.

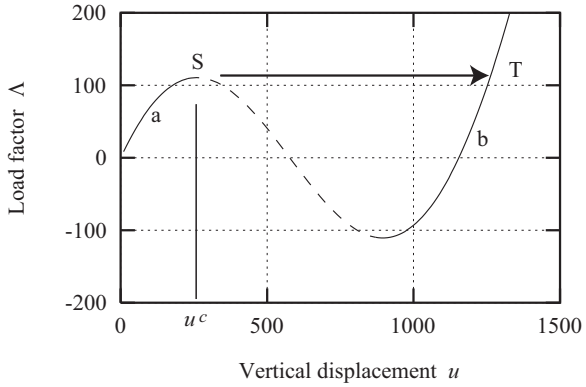

Fig. 2: Relation between u and Λ of the 2-bar truss.

Table 1: Formulations of optimization problems of a 2-bar truss.

	Objective function	Constraints
Case 1	$\min_A u(\bar{\Lambda})$	$V \le \bar{V}$
Case 2	$\min_A V$	$u(\bar{\Lambda}) \le \bar{u}$
Case 3	$\max_A \max_u \Lambda(u)$	$u \le \bar{u},\ V \le \bar{V}$

as shown in Fig. 1. A proportional load Λp is applied in y-direction at the center node. The solid and dashed lines are the members after and before deformation, respectively.

In the following examples, $W = 1000$ mm, $H = W/\sqrt{3}$, $p = 1000$ kN, and the elastic modulus E is 200 kN/mm^2. The units of force and length are kN and mm, respectively. The length of each member before deformation is denoted by L_0. The exact strain-displacement relation is used, i.e. the length L of a member after deformation is computed from the Euclid distance between the nodes, and the strain ε is defined as $(L - L_0)/L_0$. The material property is assumed to be linear elastic.

By using the symmetry condition with respect to the y-axis, the truss has only one design variable that is the cross-sectional area A of the two members. Since the inequality constraints are satisfied in equality at the optimal solutions of the following three trivial optimization problems, A is obtained directly from the constraints, and no optimization process is needed for obtaining the optimal value of A.

Let u denote the displacement in y-direction of the center node. The relation between u and Λ is as shown in Fig. 2. The limit point indicated by S is reached as Λ is increased, and the equilibrium state jumps to T after dynamic deformation called snapthrough. The solid and dashed curves indicate stable and unstable equilibrium states, respectively. The equilibrium states before the limit point and after snapthrough are indicated by 'a' and 'b', respectively. Note that the value of u at the limit point, which is denoted by $u^{\rm c}$, is independent of A in this example, and $u^{\rm c} \simeq 240.0$. Therefore, it may not be admissible to formulate a problem considering the displacement constraints at the limit point. It might seem that this independence of the displacement at the limit point on the design variables is a very special situation for this small model. However, it often happens that the critical state is strongly related to the shape of deformation. The independence or insensitivity of the deformation at the critical point on the design variables makes optimization process complicated; i.e. the responses at the critical points cannot be modified effectively by varying the design variables.

To investigate other difficulties relating to snapthrough, consider three optimization problems as listed in Table 1, where a bar indicates a specified value, and V is the total structural volume; i.e. $V = 2AL_0$. For Case 1, the displacement u at $\Lambda = \bar{\Lambda} = 1.0$ is to be minimized. Since V is an increasing function of A and $u(\bar{\Lambda})$ is a decreasing function of A, the optimal value of A is computed from $V(A) = \bar{V}$.

If $\bar{V}$ is sufficiently large, $u(\bar{\Lambda})$ is in a small range, and the optimal value of A is almost same as the geometrically linear case. The value of $u(\bar{\Lambda})$ gradually increases as $\bar{V}$ is decreased, as shown in Fig. 3, and the equilibrium state at $\Lambda = \bar{\Lambda}$ reaches the limit point at $\bar{V} = \bar{V}^{\rm S} \simeq 1.05 \times 10^5$ denoted by 'S' in Fig. 3. Note that the curves 'a' and 'b' in this figure indicate that the equilibrium state at $\Lambda = \bar{\Lambda}$ is in the regions 'a' and 'b', respectively, in Fig. 2. By further decreasing $\bar{V}$ from $\bar{V}^{\rm S}$, the equilibrium state jumps to the post-buckling state 'T' defined in Fig. 2; i.e. $u(\bar{\Lambda})$ increases discontinuously at $\bar{V} = \bar{V}^{\rm S}$. Therefore, there exist discontinuities in optimal solution and the sensitivity coefficient of $u(\bar{\Lambda})$ with respect to A, which lead to divergence of optimization process if a gradient-based optimization algorithm is used for a large structures with many members.

Consider Case 2, where an upper bound $\bar{u}$ is given for $u(\bar{\Lambda})$ and V is to be minimized. Let $\bar{\Lambda} = 1$ for simplicity. In this case, V decreases rapidly as $\bar{u}$ is increased from a small value as shown in Fig. 4 until reaching $\bar{u} = u^{\rm c}$ at 'S'. If $\bar{u} \leq u^{\rm c}$, the equilibrium state at $\Lambda = \bar{\Lambda}$ is in region 'a' defined in Fig. 2. For $\bar{u} \geq u^{\rm c}$, V has a constant value because $u(\bar{\Lambda}) = u^{\rm c}$ should be satisfied at the optimal solution. At point 'T' in Fig. 4, $\bar{u}$ reaches the value of u denoted by u^* at 'T' defined in Fig. 2. If buckling is allowed at $\Lambda < \bar{\Lambda}$, V decreases in the region $u(\bar{\Lambda}) > u^*$ as shown in the dashed curve in Fig. 4. However, if buckling is not allowed, $\bar{u} = u^{\rm c}$ should be satisfied and V has a constant value at the optimal solution for $\bar{u} > u^*$. Consequently, the optimal solution allowing buckling before reaching the final load level is quite different from the solution where buckling is not allowed.

For Case 3, the maximum value $\Lambda^{\rm M}$ of Λ in the range $u \leq \bar{u}$ is to be maximized under constraint $V \leq \bar{V}$. Fig. 5 shows the relation between $\bar{u}$ and $\Lambda^{\rm M}$ for $\bar{V} = 1.0 \times 10^5$.

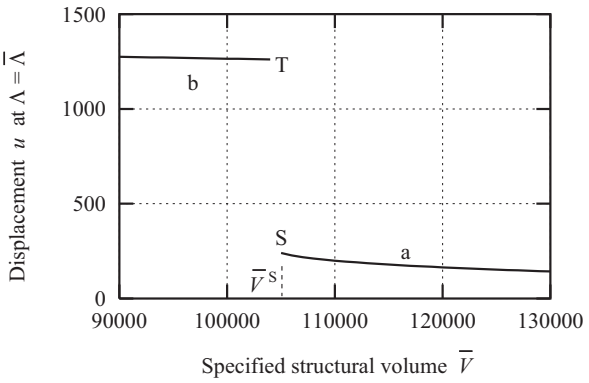

Fig. 3: Variation of the displacement u of the optimal solution of Case 1.

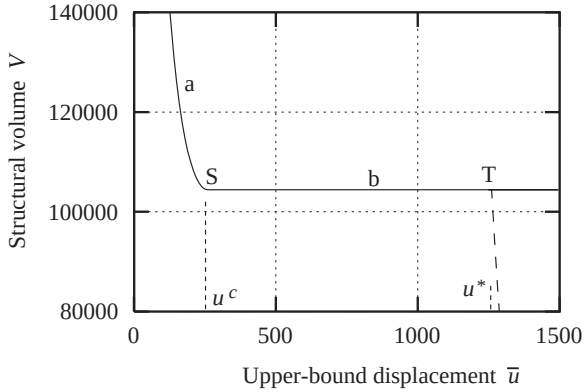

Fig. 4: Variation of the optimal structural volume of Case 2.

If $\bar{u}$ is small enough, Λ^{M} that is equal to Λ at $u = \bar{u}$ is an increasing function of $\bar{u}$ as shown in Fig. 5. However, if $u^{\mathrm{c}} \leq \bar{u} \leq u^*$, Λ^{M} has the constant value because Λ takes the maximum value at the limit point. For $\bar{u} \geq u^*$, Λ has the maximum value in region 'b' defined in Fig. 2, and Λ^{M} is an increasing function of $\bar{u}$. Note that the plot in Fig. 5 is same as that of the snapthrough behavior in Fig. 2.

3.2 Illustrative example of a 24-bar truss

Consider a 24-bar truss as shown in Fig. 6 to discuss more general situation. The numbers with and without parentheses, respectively, are the numbers of members and nodes. The nodal coordinates are as listed in Table 2. A concentrated load is applied in the negative z-direction at node 1 located at the center. Let A_i denote the cross-sectional area of the ith member. The members are divided into two groups; i.e. members 1-6 that are connected to the center node are in group 1, and the remaining members are in group 2. The cross-sectional areas are assigned by using the scalar A

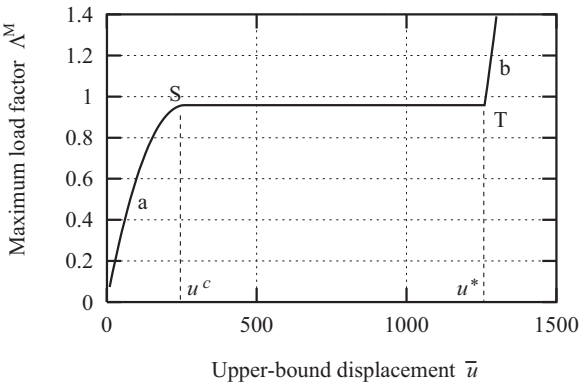

Fig. 5: Variation of the maximum load factor of the optimal solution of Case 3.

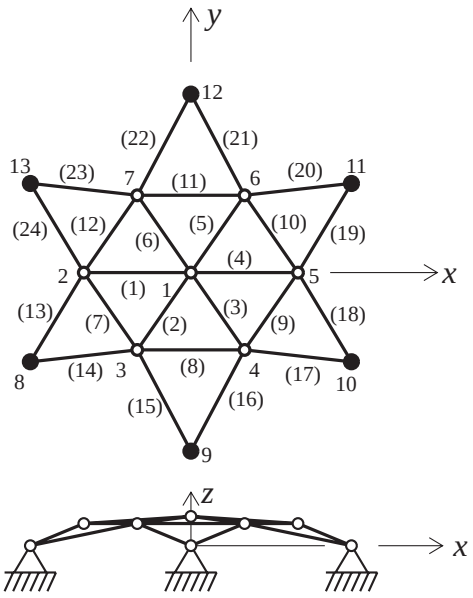

Fig. 6: A 24-bar truss.

and the ratio α as

$$\begin{aligned} A_i &= A, \quad (i = 1, 2, \ldots, 6) \\ A_i &= \alpha A, \quad (i = 7, 8, \ldots, 24) \end{aligned} \tag{10}$$

Let u denote the displacement in the negative z-direction of node 1. The relation between u and Λ for $\alpha = 1$ is plotted in Fig. 7. It can be seen from Fig. 7 that a limit point is reached as Λ is increased. Fig. 8 shows the relation between α and the displacement u^c at the limit point for designs satisfying $V = 7000$. It can be observed from Fig. 8 that u^c is very insensitive to the design modification as suggested in the example of the 2-bar truss.

Consider the same optimization problems 1-3 as listed in Table 1. For a fixed value of α, V is an increasing function of A. On the other hand, $u(\bar{\Lambda})$ and $\max_u \Lambda(u)$ are

Table 2: Nodal coordinates (mm) of the 24-bar truss.

Node Number	x	y	z
1	0.0	-5000.0	0.0
2	-4330.0	-2500.0	0.0
3	-1250.0	-2165.0	621.6
4	1250.0	-2165.0	621.6
5	4330.0	-2500.0	0.0
6	-2500.0	0.0	621.6
7	0.0	0.0	821.6
8	2500.0	0.0	621.6
9	-4330.0	2500.0	0.0
10	-1250.0	2165.0	621.6
11	1250.0	2165.0	621.6
12	4330.0	2500.0	0.0
13	0.0	5000.0	0.0

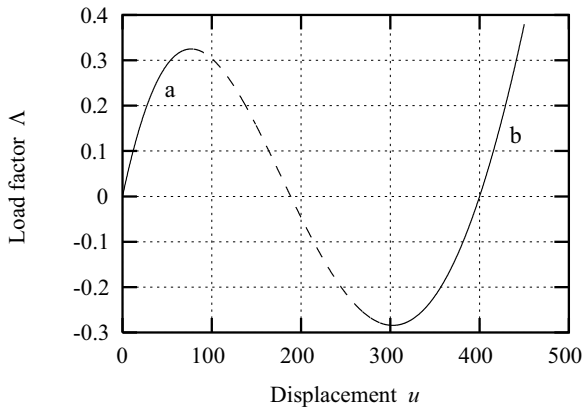

Fig. 7: Equilibrium path of the 24-bar truss for $\alpha = 1$.

non-increasing function of A. Therefore, the constraint $V \leq \bar{V}$ or $u(\bar{\Lambda}) \leq \bar{u}$ is satisfied in equality at the optimal solution, and the value of A can be obtained from the constraint for each case. This way, α can be taken as the design variable for Cases 1-3, and the properties of sensitivity coefficients of $u(\bar{\Lambda})$ and $\max_u \Lambda(u)$ with respect to α are discussed in the following.

Let $\bar{\Lambda} = 0.3$ and $\bar{V} = 7000$ for Case 1. $u(\bar{\Lambda})$ is plotted in Fig. 9 with respect to α for designs satisfying $V = \bar{V}$. It is seen from Fig. 9 that $u(\bar{\Lambda})$ is a discontinuous function of α. If α is very large, the members 1-6 around the center have small cross-sectional areas, and a limit point is reached as Λ is increased before reaching $\bar{\Lambda}$. On the other hand, if α is very small, the circumferential members 7-12 have small cross-sectional areas and members 1-6 can easily rotate. Therefore, a limit point exist at a small load level also for this case. 'a' and 'b' in Fig. 9 indicate that Λ reaches $\bar{\Lambda}$ in the regions

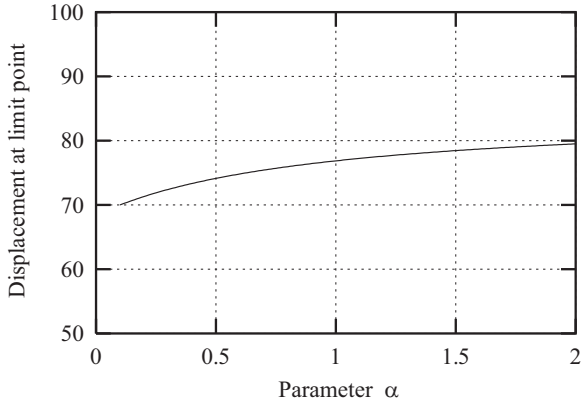

Fig. 8: Displacement at the limit point of the 24-bar truss with $V = \bar{V} = 7000$.

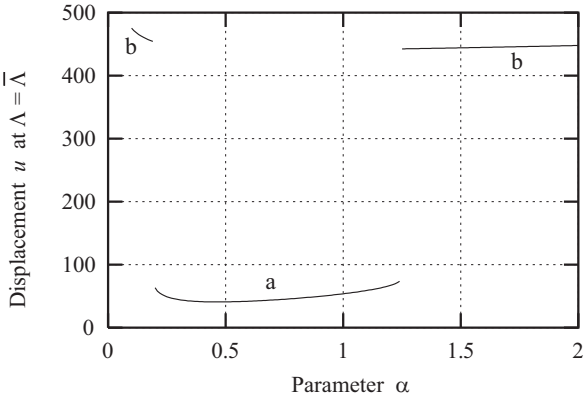

Fig. 9: Displacement at $\Lambda = \bar{\Lambda} = 0.3$ of the 24-bar truss with $V = \bar{V} = 7000$.

'a' and 'b', respectively, shown in Fig. 7. $u(\bar{\Lambda})$ has minimum value at $\alpha \simeq 0.47$ which corresponds to the optimum design.

For Case 2, the value of V satisfying the constraint $u(\bar{\Lambda}) = \bar{u}$ is a discontinuous function of α, because u at $\Lambda = \bar{\Lambda}$ for fixed V is a discontinuous function of α as observed from Fig. 9. Let $\bar{u} = 45.0$ and $\bar{V} = 7000$ for Case 3. The load factors at the limit point and at $u = 45.0$ are plotted in Fig. 10, respectively, in solid and dashed curves. Note that the limit point load coincides with Λ at $u = 45.0$ at $\alpha \simeq 0.41$, where the sensitivity coefficient of $\max_u \Lambda(u)$ with respect to α varies discontinuously. Note also that the value of u that takes the maximum value of Λ is discontinuous with respect to α at $\alpha \simeq 0.41$. Therefore, convergence of optimization method will not be guaranteed if a gradient-based method is used.

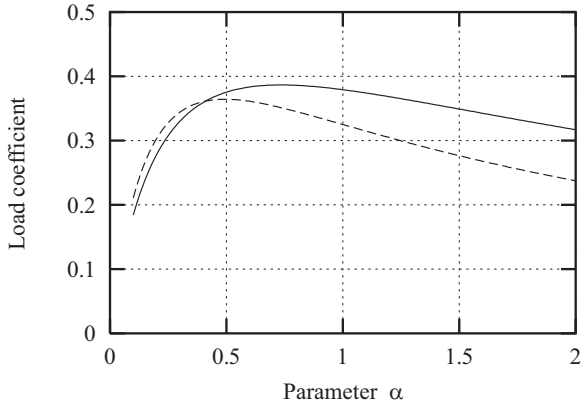

Fig. 10: Load coefficients at the limit point (solid curve) and at $u = \bar{u} = 45.0$ (dashed curve) of the 24-bar truss.

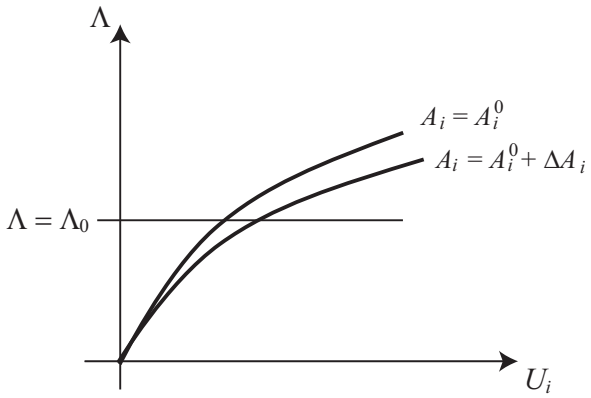

Fig. 11: Variation of equilibrium path due to design modification.

4 Sensitivity analysis of responses at the critical points.

4.1 Sensitivity analysis at regular states.

The formulations of sensitivity analysis at regular (noncritical) states are presented to provide the basic equations for sensitivity analysis at the critical points. Only elastic conservative systems are considered. The path-dependent problems with material nonlinearity can be consulted to Kleiber (25). It is known that the consistent tangent operators should be used in deriving sensitivity equations for creep problem (65) and general rate-independent elasto-plastic problem (64).

If the responses such as displacements and stresses are monotonically increasing functions of the load factor, sensitivity coefficients of nonlinear responses of elastic structures can be obtained from the information at the final load level; i.e. no incremental process is needed for design sensitivity analysis (7) although the responses

should be found incrementally or by direct iteration at the final load level if the iteration converges. Fig. 11 illustrates the variation of the equilibrium path with respect to the modification of the design variable A_i by ΔA_i from A_i^0. The purpose of design sensitivity analysis is to obtain the rate of variation of the responses at a fixed load level $\Lambda = \Lambda_0$ with respect to the variation of a design variable such as the cross-sectional area of a member or a coordinate of a node.

Let a tilde indicate partial differentiation of the explicit terms; i.e.

$$\frac{\partial \tilde{\mathbf{F}}}{\partial A_i} = \frac{\partial \mathbf{F}(\mathbf{U}, \mathbf{A})}{\partial A_i} \tag{11}$$

By differentiating (4) with respect to A_i for a fixed value of Λ, and by using (5), the following relation is derived:

$$\mathbf{K}(\mathbf{U}, \mathbf{A}) \frac{\partial \mathbf{U}(\mathbf{A})}{\partial A_i} = \Lambda \frac{\partial \tilde{\mathbf{p}}(\mathbf{A})}{\partial A_i} - \frac{\partial \tilde{\mathbf{F}}(\mathbf{U}, \mathbf{A})}{\partial A_i} \tag{12}$$

The right-hand-side terms in (12) are the differentiation of the explicit terms of $\mathbf{A}$, which can be easily obtained; e.g. $\mathbf{p}$ is a linear function of A_i if it represents the self-weight and A_i is a cross-sectional area of a member or the thickness of a plate element.

The sensitivity equation (12) at a regular state has a similar form as geometrically linear problems. However, $\mathbf{K}$ depends on $\mathbf{U}$ for geometrically nonlinear case. The equivalent nodal loads $\mathbf{F}$ is also a nonlinear function of $\mathbf{U}$, although it is a linear function of $\mathbf{U}$ for a geometrically linear case. The computation of $\mathbf{K}$ and $\mathbf{F}$ depends on the definitional of strains and stresses. The readers may consult Refs (54; 36) for the details to concentrate in this paper on sensitivity analysis and optimization related to geometrically nonlinear buckling problems.

The dependence of $\mathbf{F}$ on A_i for fixed $\mathbf{U}$ are known before constructing the element stiffness matrix. The tangent stiffness matrix $\mathbf{K}$ has been factorized at the final step of analysis. Therefore, $\dfrac{\partial \mathbf{U}(\mathbf{A})}{\partial A_i}$ can be computed from (12) within very small additional computational cost.

4.2 Sensitivity analysis at critical states.

There have been numerous number of researches for sensitivity analysis of critical loads of elastic conservative systems. The purposes of those papers are to investigate the variation of critical load with respect to initial imperfections such as material defects and manufacturing errors. On the other hand, sensitivity analysis has been developed in the field of optimization to compute the variation of the critical loads with respect to design modification. Since those results are mathematically equivalent, the valuable results in general theory of elastic stability can effectively be used in design sensitivity analysis for structural optimization (42). In this paper, we concentrate on application to structural optimization, and the topics related only to imperfection

sensitivity analysis are not included. We also exclude linear buckling loads, because there have been good review papers; e.g. by Seyranian *et al.* (57) especially for sensitivity analysis of multiple buckling loads.

Sensitivity coefficients of limit point loads can be found easily only from the equilibrium equations. By differentiating (4) with respect to A_i at the limit point $\Lambda = \Lambda^{\mathrm{c}}$ and by considering Λ^{c} as function of A_i, the following relation is derived:

$$\mathbf{K}\frac{\partial \mathbf{U}}{\partial A_i} = \frac{\partial \Lambda^{\mathrm{c}}}{\partial A_i}\mathbf{p} + \Lambda^{\mathrm{c}}\frac{\partial \tilde{\mathbf{p}}}{\partial A_i} - \frac{\partial \tilde{\mathbf{F}}}{\partial A_i} \tag{13}$$

where (5) has been used. By premultiplying the lowest eigenmode Φ_1^{c} to the both sides of (13), and by using $\lambda_1 = 0$ at the limit point for (6), the sensitivity coefficient of the limit point load is obtained as

$$\frac{\partial \Lambda^{\mathrm{c}}}{\partial A_i} = \frac{\Phi_1^{\mathrm{c}\top}\dfrac{\partial \tilde{\mathbf{F}}}{\partial A_i} - \Lambda^{\mathrm{c}}\Phi_1^{\mathrm{c}\top}\dfrac{\partial \tilde{\mathbf{p}}}{\partial A_i}}{\Phi_1^{\mathrm{c}\top}\mathbf{p}} \tag{14}$$

Note from (9) that the denominator of (14) vanishes at a bifurcation point. Therefore, (14) is valid only for a limit point (47), and the sensitivity coefficients of the limit point load can be found without computing the sensitivity coefficients of displacements as observed from (14).

There have been many studies on design sensitivity analysis of critical load factors. However, the sensitivity equations derived for the limit point loads are essentially same as those derived in the field of stability analysis of elastic conservative systems (59; 61). Furthermore, there have been numerous number of papers on imperfection sensitivity analysis of bifurcation loads.

It is important to note that the bifurcation points usually exist in the case where the structure to be designed has a symmetry property. Therefore, for the purpose of optimum design, only symmetric design modification, which is regarded as a special type of imperfection, should be considered for calculating sensitivity coefficients. Fig. 12 illustrates symmetric and antisymmetric design modification of a symmetric frame that can be conceived as initial imperfections.

Suppose the initial perfect symmetric system has a bifurcation point. For a design modification corresponding to symmetric imperfection, the critical point of a modified symmetric structure is still a bifurcation point as illustrated in Fig. 13, where the dashed line and curve are the fundamental equilibrium path and the bifurcation path of the original *perfect* structure, respectively, and the solid curves are the bifurcation paths of the modified *imperfect* structures. The horizontal axis U_a represents an antisymmetric component of displacements. Since the bifurcation path is symmetric with respect to Λ-axis and Λ decreases along the bifurcation path, this bifurcation point is called symmetric unstable bifurcation point. The imperfection that preserves the bifurcation property is categorized as *minor imperfection* or *second order imperfection* (53; 61), and the variation of the bifurcation load factor is a linear function of the imperfection parameter.

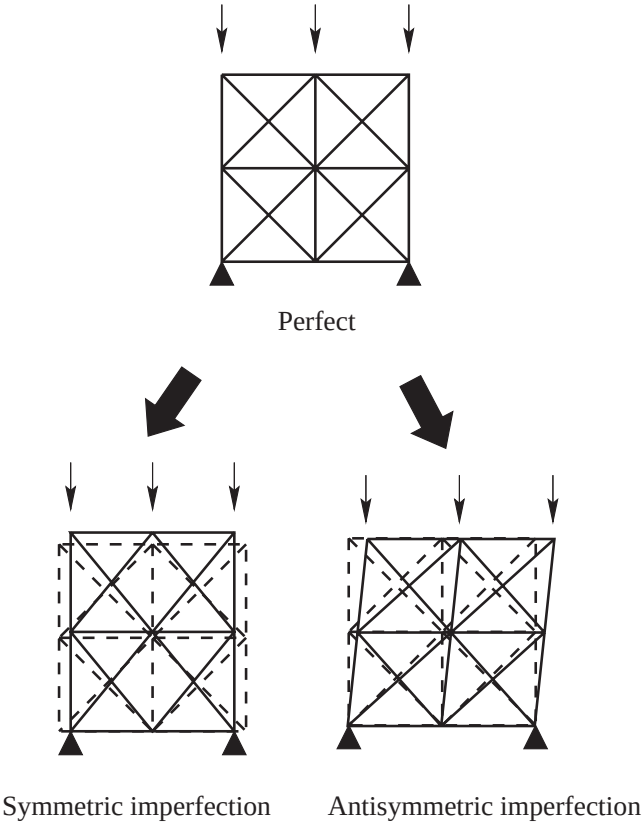

Fig. 12: Classification of imperfections that are considered as design modifications.

On the other hand, for a design modification corresponding to asymmetric imperfection, the critical point of a modified antisymmetric structure is a limit point as illustrated in Fig. 14 if the bifurcation point of the perfect structure is symmetric and unstable. In this case, the imperfection is called *major imperfection* or *first order imperfection*, and imperfection sensitivity of the critical load factor is infinity given by the well-known 2/3-power law (26). Sensitivities relating to minor and major imperfections, respectively, are also called *regular sensitivity* and *singular sensitivity* (34). If the bifurcation point is stable, the critical point along the fundamental path disappears as discussed in Section 6. Suppose we formulate an optimization problem to maximize the bifurcation load factor. A path-following analysis to find the bifurcation load should be carried out at each iterative step of optimization. However, the analysis may not stop if asymmetric design modification is allowed. Therefore, the feasible design should be strictly limited to be symmetric to prevent any divergence in the optimization process.

Since sensitivity analysis of bifurcation loads with respect to minor imperfection is practically important for application to structural optimization, two methods are briefly presented in the following.

Fig. 15 illustrates the variations of λ_1 for designs defined by $A_i = A_i^0$ and $A_i = A_i^0 + \Delta A_i$. Since the bifurcation load factor Λ^c is defined as the value of Λ at which

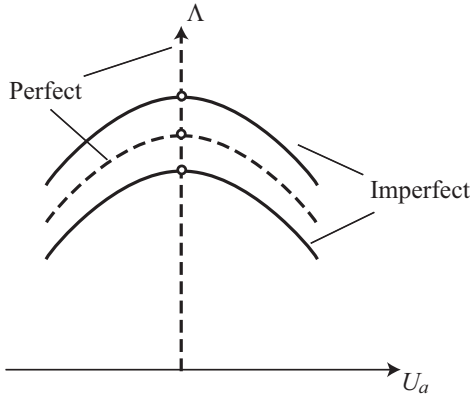

Fig. 13: Equilibrium paths of imperfect systems corresponding to symmetric imperfections for an unstable symmetric bifurcation point.

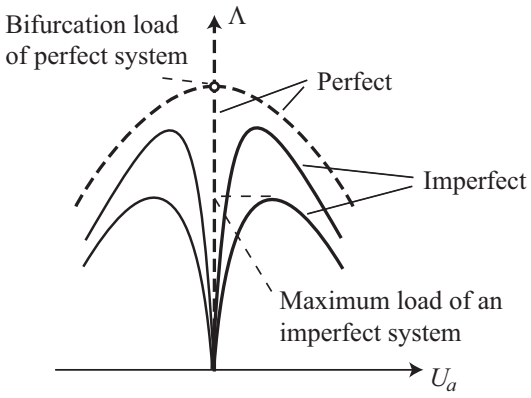

Fig. 14: Equilibrium paths of imperfect systems corresponding to asymmetric imperfections for an unstable symmetric bifurcation point.

$\lambda_1 = 0$ is satisfied, the sensitivity of Λ^{c} can be obtained as the differential coefficient of Λ under constraint $\lambda_1 = 0$. Consider first a general case of $\lambda_1 \neq 0$, and let λ^* denote the specified value for λ_1. The values corresponding to $\lambda_1 = \lambda^*$ are denoted by $(\ )^*$. By differentiating (5)-(7) with respect to A_i for $\lambda_1 = \lambda^*$, the following relations are derived (43):

$$\frac{\partial \tilde{\mathbf{F}}}{\partial A_i} + \mathbf{K}^* \frac{\partial \mathbf{U}^*}{\partial A_i} = \Lambda^* \frac{\partial \tilde{\mathbf{p}}}{\partial A_i} + \frac{\partial \Lambda^*}{\partial A_i} \mathbf{p} \tag{15}$$

$$\frac{\partial \tilde{\mathbf{K}}}{\partial A_i} \Phi_1^* + \sum_{j=1}^{n} \frac{\partial \mathbf{K}}{\partial U_j} \frac{\partial U_j^*}{\partial A_i} \Phi_1 + \mathbf{K}^* \frac{\partial \Phi_1^*}{\partial A_i} = \lambda^* \frac{\partial \Phi_1^*}{\partial A_i} \tag{16}$$

$$2 \Phi_1^{*\top} \frac{\partial \Phi_1^*}{\partial A_i} = 0 \tag{17}$$

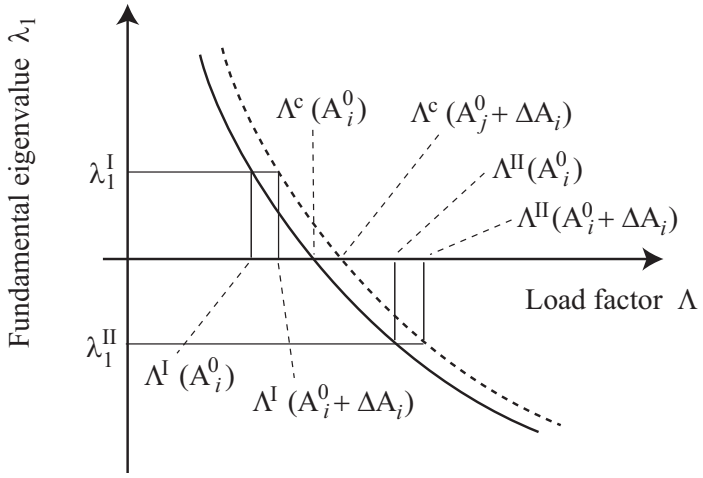

Fig. 15: Variation of bifurcation point defined by interpolation.

Note that Λ^*, $\mathbf{U}^*$ and Φ_1^* are considered as function of A_i, and the sensitivity coefficients $\dfrac{\partial\Lambda^*}{\partial A_i}$, $\dfrac{\partial\mathbf{U}^*}{\partial A_i}$ and $\dfrac{\partial\Phi_1^*}{\partial A_i}$ for fixed λ_1 can be obtained from (15)-(17), because we have $2n+1$ unknowns and $2n+1$ linear equations. However, since $\mathbf{K}$ is singular at a critical point, the set of equations (15)-(17) are singular at the bifurcation point (44).

Several methods have been presented for preventing this singularity. Ohsaki and Uetani (43) presented an interpolation technique to find the sensitivity coefficients of the bifurcation load factor Λ^{c}. Let Λ^{I} and Λ^{II} denote two load factors near Λ^{c} satisfying $\lambda_1(\Lambda^{\mathrm{I}})>0$ and $\lambda_1(\Lambda^{\mathrm{II}})<0$ as illustrated in Fig. 15. For simplicity, define the eigenvalues as $\lambda_1^{\mathrm{I}}=\lambda_1(\Lambda^{\mathrm{I}})$, $\lambda_1^{\mathrm{II}}=\lambda_1(\Lambda^{\mathrm{II}})$. The value of Λ^{c} is approximated by interpolation as

$$\Lambda^{\mathrm{c}} \simeq \frac{\lambda_1^{\mathrm{I}}\Lambda^{\mathrm{II}}-\lambda_1^{\mathrm{II}}\Lambda^{\mathrm{I}}}{\lambda_1^{\mathrm{I}}-\lambda_1^{\mathrm{II}}} \tag{18}$$

By differentiating (18) for fixed values of λ^{I} and λ^{II},

$$\frac{\partial\Lambda^{\mathrm{c}}}{\partial A_i} \simeq \frac{\lambda_1^{\mathrm{I}}\dfrac{\partial\Lambda^{\mathrm{II}}}{\partial A_i}-\lambda_1^{\mathrm{II}}\dfrac{\partial\Lambda^{\mathrm{I}}}{\partial A_i}}{\lambda_1^{\mathrm{I}}-\lambda_1^{\mathrm{II}}} \tag{19}$$

is obtained. Hence $\dfrac{\partial\Lambda^{\mathrm{c}}}{\partial A_i}$ can be found from $\dfrac{\partial\Lambda_1^{\mathrm{I}}}{\partial A_i}$ and $\dfrac{\partial\Lambda_1^{\mathrm{II}}}{\partial A_i}$ that can be computed from (15)-(17) by incorporating $\lambda^*=\lambda_1^{\mathrm{I}}$ and $\lambda^*=\lambda_1^{\mathrm{II}}$, respectively. The accuracy within more than five digits of (19) has been confirmed in Ref. (43).

Note that the second term in the left-hand-side of (16) is the differentiation of matrix $\mathbf{K}$ with respect to the vector $\mathbf{U}$, which is equivalent to third order differentiation of the total potential energy. Computation of third order differential coefficients requires substantial computational cost and large effort for programming (9; 51). In the

practical situation, the responses of geometrically nonlinear structures are computed by an incremental approach that utilizes tangent stiffness which is the second order differential coefficients of the total potential energy. Therefore, it is practically useful if computation of third order terms can be avoided.

The second term in the left-hand-side of (16) can be rewritten as

$$\sum_{j=1}^{n} \frac{\partial \mathbf{K}}{\partial U_j} \frac{\partial U_j}{\partial A_i} \Phi_r = \sum_{j=1}^{n} \frac{\partial (\mathbf{K}\Phi_r)}{\partial U_j} \frac{\partial U_j}{\partial A_i} \tag{20}$$

and a finite difference approach can be used for sensitivity computation of the vector $\mathbf{K}\Phi_r$ at element level with respect to U_j, which is known as *semi-analytical approach* (12; 9). Reitinger *et al.* (51) presented a semi-analytical approach for sensitivity analysis of critical loads, and developed an optimization algorithm considering the effect of initial imperfection. Mróz and Haftka (34) also derived rigorous forms of sensitivity analysis of limit point loads and bifurcation loads. Examples of optimum design with limit points have been presented in Mróz and Piekarski (35). In their approach, computation of the third order differentiation of the total potential energy is also required for bifurcation loads.

Another approach for avoiding singularity of $\mathbf{K}$ is to linearly estimate the bifurcation point from a moderately smaller load level (67; 37). The tangent stiffness matrix can be divided into linear part $\mathbf{K}_{\mathrm{L}}(\mathbf{A})$ and nonlinear part $\mathbf{K}_{\mathrm{N}}(\Lambda, \mathbf{A})$. Then the eigenvalue problem is written as

$$[\mathbf{K}_{\mathrm{L}}(\mathbf{A}) + \mathbf{K}_{\mathrm{N}}(\Lambda^{\mathrm{c}}, \mathbf{A})]\Psi = \mathbf{0} \tag{21}$$

where Ψ is normalized as

$$\Psi^{\top} \mathbf{K}_{\mathrm{L}} \Psi = 1. \tag{22}$$

Note that Ψ is not normalized by $\mathbf{K}_{\mathrm{N}}$ because $\mathbf{K}_{\mathrm{N}}$ is not positive or negative definite.

Let Λ^* denote a load factor that is moderately smaller than Λ^{c}. Assume $\mathbf{K}_{\mathrm{N}}(\Lambda, \mathbf{A})$ can be linearly estimated with respect to Λ at $\Lambda = \Lambda^*$ as

$$\mathbf{K}_{\mathrm{N}}(\Lambda, \mathbf{A}) = \frac{\Lambda}{\Lambda^*} \mathbf{K}_{\mathrm{N}}(\Lambda^*, \mathbf{A}) \tag{23}$$

and let $\mu = \Lambda / \Lambda^*$. Then (21) is rewritten as

$$[\mathbf{K}_{\mathrm{L}}(\mathbf{A}) + \mu^{\mathrm{c}} \mathbf{K}_{\mathrm{N}}(\Lambda^*, \mathbf{A})]\Psi = \mathbf{0} \tag{24}$$

where $\mu^{\mathrm{c}} = \Lambda^{\mathrm{c}} / \Lambda^*$.

By differentiating (24) with respect to A_i, and by using (24) and (22), the following equation is derived:

$$\begin{aligned} \frac{\partial \mu^{\mathrm{c}}}{\partial A_i} = {} & \mu^{\mathrm{c}} \Psi^{\top} \frac{\partial \mathbf{K}_{\mathrm{L}}}{\partial A_i} \Psi + \mu^{\mathrm{c}} \Psi^{\top} \sum_{j=1}^{n} \frac{\partial (\mathbf{K}_{\mathrm{L}} \Psi)}{\partial U_j} \frac{\partial U_j}{\partial A_i} \\ & + (\mu^{\mathrm{c}})^2 \Psi^{\top} \frac{\partial \tilde{\mathbf{K}}_{\mathrm{N}}}{\partial A_i} \Psi + (\mu^{\mathrm{c}})^2 \Psi^{\top} \sum_{j=1}^{n} \frac{\partial (\mathbf{K}_{\mathrm{N}} \Psi)}{\partial U_j} \frac{\partial U_j}{\partial A_i} \end{aligned} \tag{25}$$

Note that $\dfrac{\partial U_j}{\partial A_i}$ can be computed from (12). The derivatives of the matrix $\mathbf{K}$ need not be computed, and only the derivatives of the vectors $\mathbf{K}_{\mathrm{L}}\Psi$ and $\mathbf{K}_{\mathrm{N}}\Psi$ should be computed, where a semi-analytical approach can be effectively used. However, (24) is an approximate relation neglecting the difference of deformation shape between $\Lambda = \Lambda^*$ and $\Lambda = \Lambda^{\mathrm{c}}$. Furthermore, the choice of the appropriate value of Λ^* will be very difficult.

If Ψ can be assumed to be independent of $\mathbf{U}$, which is not correct in general, the second term in the right hand side of (25) vanishes, and the fourth term can be approximated as

$$\mu^{\mathrm{c}}\Psi^{\top}\sum_{j=1}^{n}\frac{\partial(\mathbf{K}_{\mathrm{N}}\Psi)}{\partial U_j}\frac{\partial U_j}{\partial A_i} \simeq \mu^{\mathrm{c}}\sum_{j=1}^{n}\Psi^{\top}\frac{\partial(\mathbf{K}_{\mathrm{N}})}{\partial U_j}\Psi\frac{\partial U_j}{\partial A_i} \tag{26}$$

Since $\mathbf{K}_{\mathrm{N}}$ is a function of internal forces or stresses, $\dfrac{\partial(\mathbf{K}_{\mathrm{N}})}{\partial U_j}$ can be computed easily in an element level.

Noguchi and Hisada (36) developed a sensitivity analysis method compatible to a cylindrical arc-length method (8) for tracing the equilibrium path. In their method, $\Phi_1^{\mathrm{c}\top}$ in (14) is replaced by $\mathbf{v}$ defined by

$$\mathbf{v} = \mathbf{K}^{-1}\Delta\mathbf{U} \tag{27}$$

where $\Delta\mathbf{U}$ is the displacement increment in the process of tracing the equilibrium path. Since $\mathbf{K}$ is singular at the critical point, $\mathbf{v}$ should be evaluated at the equilibrium state near the critical point. Kwon *et al.* (30) extended this approach to be compatible with one- and two-point approximations for detecting the critical points along the equilibrium path by incremental approach.

It should be noted here again that the design modification or imperfection given for applying any of the design sensitivity analysis method of bifurcation loads shown in this section should correspond to a minor imperfection. Otherwise, the critical point of the modified or imperfect structure is a limit point, and obviously the sensitivity coefficients are infinity (61); i.e. the critical loads of imperfect systems should be estimated by 1/2- or 2/3-power law.

5 Difficulties in optimization of geometrically nonlinear structures.

Difficulties in optimization against buckling are mainly related to discontinuities in design sensitivity coefficients. The difficulties corresponding to the snapthrough behavior have been demonstrated in Section 3. Discontinuous properties have been extensively studied for linear buckling loads (14; 57), and optimality criteria methods have been developed for optimization under multiple eigenvalue constrains. Discontinuity can be successfully avoided if the SDP problems are successively solved (22; 29).

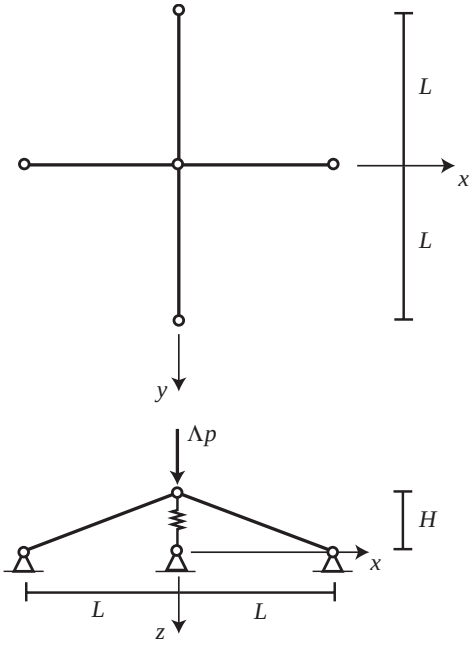

Fig. 16: A 4-bar truss with spring.

For nonlinear buckling problems, difficulties also exist due to multiple buckling loads, which are called *coincident critical points* or *compound branching* (63). Ohsaki (38) showed that optimization usually leads to a structure with coincident critical points, and several bifurcation points are located at the limit point for a shallow latticed dome. The coincident critical points of this type are called *hill-top branching points* (60; 20; 41).

To demonstrate discontinuities in optimum design with respect to the problem parameters, and in sensitivity coefficients with respect to the design variables, optimum designs are found for a 4-bar truss as shown in Fig. 16. The truss has four symmetrically located bars and a vertical spring attached at the center node. Let $L = 1000$ mm, $E = 200$ GPa, $p = 1000$ kN. The units of force and length are kN and mm also for this example. The extensional stiffness of the spring is denoted by D. The exact strain-displacement relation is used. The four members have the same cross-sectional area A, and the truss is symmetric with respect to the xz-plane and yz-plane. The total structural volume V is to be minimized under constraints on the critical load factor. Only the height H is chosen as design variable. The critical point is a limit point if H is sufficiently small, and is a bifurcation point if H has a moderately large value.

Consider the truss without spring; i.e. $D = 0$. First we fix A to investigate the relation between H and Λ^{c}. Fig. 17 shows the relation between H and Λ^{c} for $A = 100$. It is observed from Fig. 17 that Λ^{c} increases as H is increased from 1500, because the critical point is a limit point, and the snapthrough behavior may be prevented if H has a larger value. At $H = H^* \simeq 1540$, the truss has a hill-top branching point that has a bifurcation point at the limit point. In the range $H > H^*$, the bifurcation

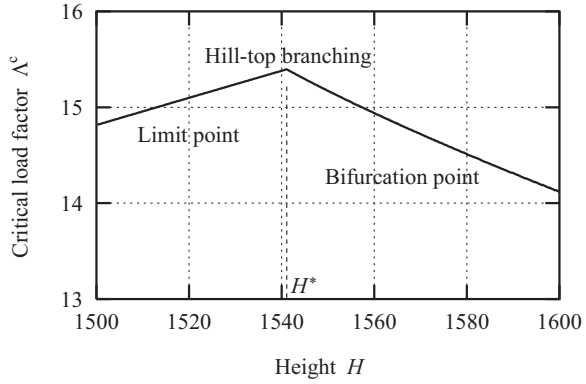

Fig. 17: Relation between height and critical load factor of the 4-bar truss with constant cross-sectional area ($D = 0$).

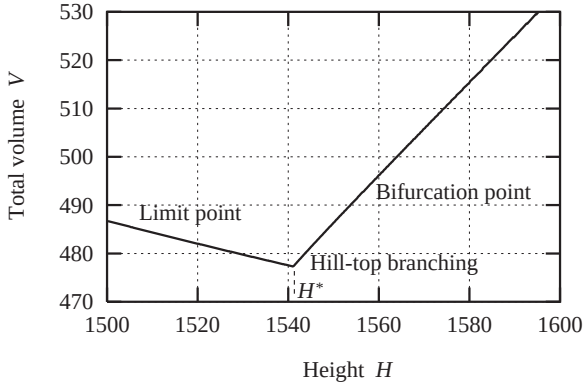

Fig. 18: Relation between height and structural volume of the 4-bar truss with constant cross-sectional area ($D = 0$).

load factor decreases as H is further increased because stiffness decreases against the bifurcation mode with lateral displacement of the center node.

Suppose a constraint is given as

$$\Lambda^{\mathrm{c}} = 1 \tag{28}$$

Since Λ^{c} is an increasing function of A, the value of A can be calculated directly from (28) for each value of H. Fig. 18 shows the relation between H and V satisfying (28). It is seen from Figs. 17 and 18 that $H = H^*$ is the optimal solution, because V has the minimum value, and a truss that has a hill-top branching point is obtained as a result of optimization.

The eigenvalues of the tangent stiffness matrix are plotted in Fig. 19 with respect to the displacement w in z-direction at the center node of the optimal solution. Note that the eigenvalue corresponding to the bifurcation type buckling decreases to 0 at the hill-top branching point, but increases to positive values as w is further increased.

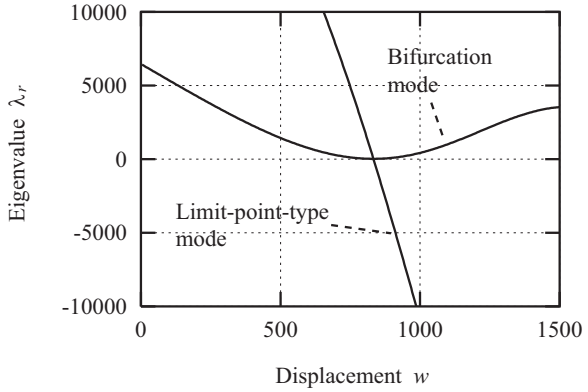

Fig. 19: Relation between displacement and eigenvalues of the optimal 4-bar truss ($D = 0$).

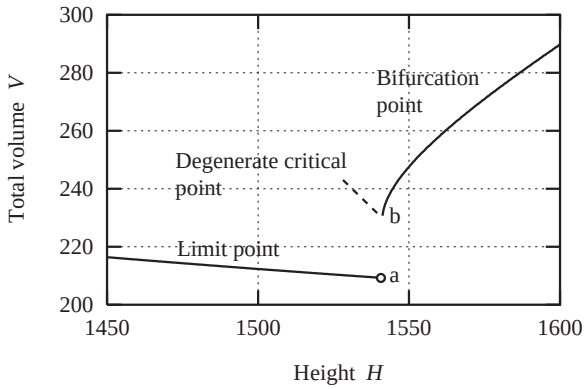

Fig. 20: Relation between height and structural volume of the 4-bar truss with spring ($D = 20$).

The bifurcation point of this type is called *degenerate critical point*. Therefore, in this case, the optimal solution has a *degenerate hill-top branching point* (38; 39).

If a gradient based optimization algorithm is used, we have to assume that the optimal solution and the intermediate solutions during optimization of complex structures may have coincident and/or degenerate critical points. Since the design sensitivity of the degenerate critical point is unbounded even for a design modification corresponding to a minor imperfection as illustrated in the following example, this fact leads to a serious difficulty in optimization by mathematical programming approach.

To illustrate an optimal solution with degenerate critical point, consider next a 4-bar truss with spring, where $D = 20$ kN/mm. Fig. 20 shows the relation between H and V satisfying (28). The truss has a degenerate critical point at 'b', where $H = H^* \simeq 1540$, and the blank circle at 'a' indicates this point is not included in the plot, i.e. V is a discontinuous function of H at $H = H^*$. Fig. 21 shows the relation between the eigenvalues of the tangent stiffness matrix and w for $H = H^*$. Note that the eigenvalue corresponding to the bifurcation type buckling decreases to 0 at 'b' before reaching

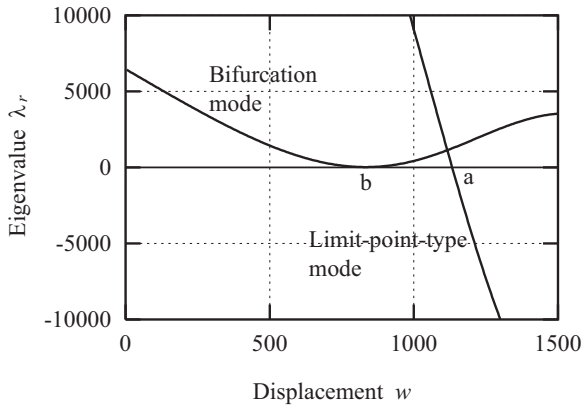

Fig. 21: Relation between displacement and eigenvalues of the optimal 4-bar truss with spring ($D = 20$).

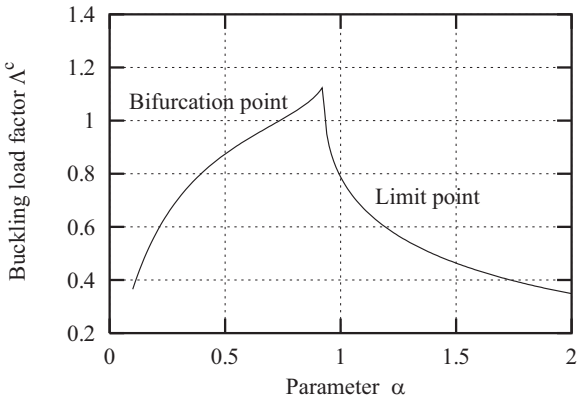

Fig. 22: Relation between buckling load factor and parameter α of the 24-bar truss.

the limit point 'a', but increases as w is further increased. The degenerate critical point at 'b' disappears if H is slightly decreased from H^* and the lowest critical point jumps to point 'a' in Fig. 21. Therefore, the sensitivity coefficient of Λ^c with respect to H is unbounded at $H = H^*$. Based on rigorous mathematical definition, there is no optimal solution for this problem, because the truss with degenerate critical point is located at the boundary of an open domain. Since the degenerate critical point is not sensitive to an imperfection, as shown in the following section, the value of H that is slightly smaller than H^* is regarded as an optimal solution from the engineering point of view.

Consider again the 24-bar truss as shown in Fig. 6 with uniformly distributed load; i.e. $p_i = -1.0$ for nodes 1-7, where p_i denotes the load in z-direction at node i. Suppose the constraint is given as $V = 7000$ and we maximize the nonlinear buckling load factor Λ^c. The parameter α is used for defining the ratios of cross-sectional areas as (10) also for this example. Fig. 22 shows the relation between Λ^c and α. If α is small, the critical point is a bifurcation point, whereas the critical point is a limit point

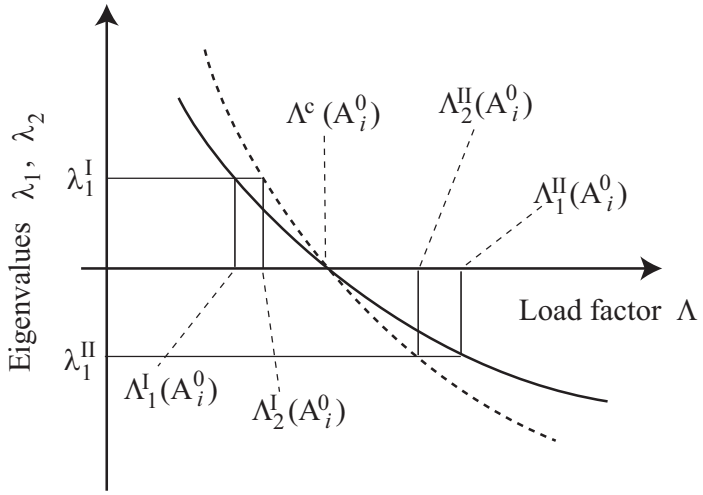

Fig. 23: Interpolation for coincident critical points.

if α is large. At $\alpha \simeq 0.92$, the limit point and the bifurcation point coincide and Λ^{c} takes the maximum value; i.e. the optimum solution has a hill-top branching point.

At the coincident critical points, methods of sensitivity analysis and optimization for simple critical point cannot be used, because the eigenmodes of the tangent stiffness matrix cannot be determined uniquely from (6). If the interpolation approach (18) is used, nonuniqueness of the eigenmode can be avoided because the eigenvalues λ_r of the tangent stiffness matrix do not exactly coincide at the two load levels Λ^{I} and Λ^{II}, respectively, below and above the coincident critical points as illustrated in Fig. 23. In this case, two sets of load factors $(\Lambda_1^{\mathrm{I}}, \Lambda_1^{\mathrm{II}})$ and $(\Lambda_2^{\mathrm{I}}, \Lambda_2^{\mathrm{II}})$ can be defined based on continuity of the eigenmodes. Symmetry properties of the modes can be used effectively. Then the sensitivity coefficient of critical load factor can be computed from (19) for each mode (38). Note that the hill-top branching points can not be found by the load increment method. In this case, the parameter Λ should be replaced by another parameter such as nodal displacement or arc-length parameter (38).

6 Imperfection sensitivity of optimal solution.

If a structure has an unstable symmetric bifurcation point, the maximum load is drastically reduced from the bifurcation load as illustrated in Fig. 14 due to small initial asymmetric imperfection corresponding to inevitable errors in nodal locations and material defects in manufacturing and fabrication processes. The structures of this type is said to be *imperfection sensitive*. It is known that maximum loads of shells and latticed frames found by experiments are far below the theoretical estimate of the bifurcation loads of the perfect systems. Extensive research has therefore been done on imperfection sensitivity analysis since the pioneering work by Koiter (26).

For optimization problems under constraints on bifurcation loads, the reduction of maximum load can be incorporated in the formulation of optimization problem by

utilizing the well-known formula of imperfection sensitivity based on the perturbation theory (51; 44). Let ξ denote the parameter defining the magnitude of imperfection. The vector of initial imperfection such as dislocation of nodes is defined by ξ and the mode vector $\mathbf{b}$ as $\xi\mathbf{b}_0$. Then the maximum load $\Lambda^{\mathrm{M}}(\xi)$ of an imperfect structure exhibiting unstable symmetric bifurcation is defined by using the bifurcation load Λ_0^{c} of the perfect structure and the coefficient $C(\mathbf{b}_0, \mathbf{A}) > 0$ as

$$\Lambda^{\mathrm{M}}(\xi) = \Lambda_0^{\mathrm{c}} - C(\mathbf{b}_0, \mathbf{A})\xi^{\frac{2}{3}} \tag{29}$$

It is seen from (29) that the reduction of maximum load is proportional to $\xi^{\frac{2}{3}}$ and the coefficient is a function of the design variable $\mathbf{A}$ and the imperfection mode $\mathbf{b}_0$. The imperfection mode that reduces the maximum load most drastically for a given norm is called *critical imperfection* (18).

The maximum load reduced due to the critical imperfection of the possible norm can be incorporated in the formulation of the optimization problem (44; 58). However, it is not practically acceptable to derive analytical form of critical imperfection from (29) and differentiate it to find the sensitivity coefficients. Therefore, a semi-analytical approach may be used, or the sensitivity of $C(\mathbf{b}_0, \mathbf{A})$ can be simply neglected in the optimization process (44).

Note that the 2/3-power law in (29) does not mean that the reduction of the maximum load for the imperfection with the norm of practical interest is always large. Obviously, the reduction will be small if the coefficient $C(\mathbf{b}_0, \mathbf{A})$ is sufficiently small. Ohsaki (40) pointed out that a minor (symmetric) imperfection is sometimes more critical than the major (asymmetric) imperfection. Therefore reduction of the bifurcation load due to a minor imperfection should also be incorporated in the problem formulation.

It is well known that imperfection sensitivity is further enhanced by interaction of buckling modes corresponding to coincident critical points (63; 17; 16). Danger in optimizing imperfection sensitive structures against buckling has been widely discussed (62; 46). Interaction between local and global modes are also important for framed structures (28; 27) and composite structures (31). The effect of interaction is theoretically defined by using the third and fourth order differential coefficients of the total potential energy, which is summarized as

1. Let Φ^{A} and Φ^{B} denote two bifurcation modes corresponding to coincident bifurcation points. Suppose Φ^{A} and Φ^{B} are related to asymmetric and symmetric bifurcation and interaction between the two modes cannot be neglected. In this case, the structure is said to be *semi-symmetric* (63; 17). Then an imperfection in the direction of Φ^{A} leads to a minor imperfection for Φ^{B}, and the bifurcation load corresponding to Φ^{B} is drastically reduced as the deformation in the direction of Φ^{A} is rapidly increased; i.e. a bifurcation point may exist before reaching the limit point along the equilibrium path of an imperfect system. Interaction of this type is called *third order interaction*.

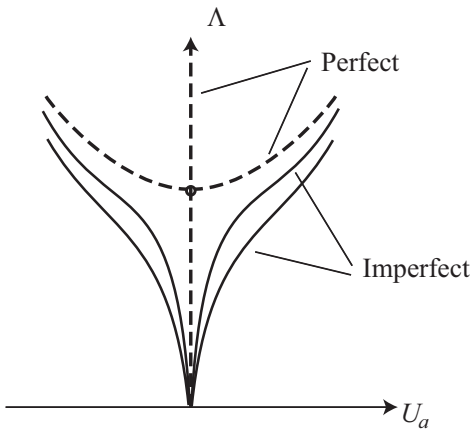

Fig. 24: Equilibrium paths of imperfect systems corresponding to a stable symmetric bifurcation point.

2. Consider a structure that has two symmetric bifurcation points, and suppose the bifurcation paths are stable if the two bifurcation points do not coincide; i.e. the fourth order differential coefficients of the total potential energy in the directions of bifurcation modes are positive. If a cross-term of the fourth differential coefficient is negative, there may be an unstable secondary bifurcation point along the bifurcation path near the first bifurcation point. In this case, another pair of bifurcation paths can exist if two bifurcation points coincide, and the new paths may be unstable due to interaction of two modes. Interaction of this type is called *fourth order interaction* that can be observed in a simple example called Augusti model (63).
3. Consider a thin-walled shell or a frame structure. Suppose the critical load factors corresponding to local mode Φ^{L} and global mode Φ^{G} coincide. Then an imperfection in the direction of Φ^{L} leads to rapid increase of deformation in the direction of Φ^{L}, which is also regarded as imperfection for Φ^{G}. Consequently, deformation in the direction of Φ^{G} increases, and as a result the deformation in the direction of Φ^{L} is enhanced. By continuing this process, the maximum load factor is drastically reduced. This interaction of local and global modes should be classified as third or fourth order interaction.

Although it is widely recognized that the coincidence of critical points may lead to an extremely imperfection sensitive structure, it should be noted here that they are not always imperfection sensitive. For shallow space trusses, optimization leads to hill-top branching, as demonstrated in Section 5, where several bifurcation points exist at a limit point (43). It has been shown, however, the hill-top branching point is not imperfection sensitive (60; 20; 19); i.e. the maximum load factor of imperfect structure are piecewise linear function of the imperfection parameter. Therefore, the maximum loads can be effectively increased by optimizing the perfect system against nonlinear buckling loads (38).

Another difficulty arises for the case of stable bifurcation. Fig. 24 illustrates the fundamental equilibrium paths and bifurcation paths of perfect and imperfect systems

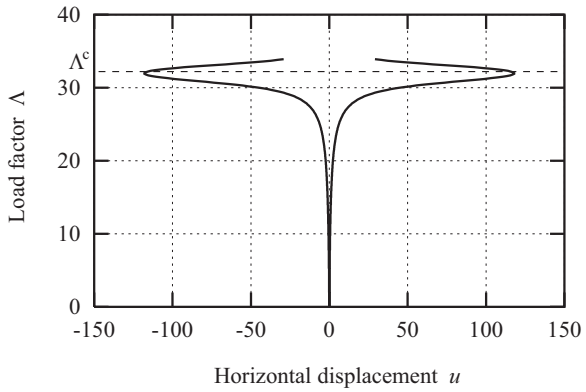

Fig. 25: Relation between displacement and load factor of the imperfect optimal 4-bar truss with spring.

corresponding to a major imperfection for the case where the perfect system has a stable symmetric bifurcation point. The horizontal axis U_a represents an antisymmetric component of displacements. It is seen from Fig. 24 that the critical point disappears due to a major imperfection. Therefore, there may be several possibilities as follows to formulate an optimization problem that has stable symmetric bifurcation points (40):

1. Existence of stable bifurcation point may be allowed before reaching the specified load level $\bar{\Lambda}$, because there always exist asymmetric initial imperfection and Λ can reach $\bar{\Lambda}$ without experiencing any unstable behavior.
2. The maximum load should be defined by the constraints on displacements and/or stresses. Therefore, constraints on buckling load are not necessary.
3. Even if the bifurcation point is stable, the deformation above the bifurcation load of an imperfect system may me unexpectedly large, because real deformation process is dynamic. In this case, the constraints on buckling loads should be incorporated.

Stable optimal solutions can be found by introducing constraints on stability of the bifurcation points that are defined by the fourth-order differential coefficients of the total potential energy (48; 4; 11; 5).

It has been shown in the previous section that existence of a degenerate critical point leads to serious difficulty in optimization process due to discontinuity in design sensitivity coefficients. However, in practical point of view, degenerate critical point may cause no serious trouble. For example, consider again the optimal 4-bar truss with spring ($D = 20\,\mathrm{kN/mm}$) as shown in Fig. 16, where the relation between λ_r and w has been plotted in Fig. 21. The perfect system has a degenerate critical point at $\Lambda \simeq 32.0$. Imperfections of $\pm 1.0\,\mathrm{mm}$ have been given in x-direction at the center node of the truss. Fig. 25 shows the relation between Λ and the displacement u in x-direction of the center node. It is seen from Fig. 25 that u has a very large value around the degenerate critical point. However, the absolute value of u decreases as Λ is further increased. Therefore, the structure is stable, and there is no bifurcation path or snapthrough behavior. The existence of degenerate critical point can be neglected if the deformation along the equilibrium path is within the specified tolerance.

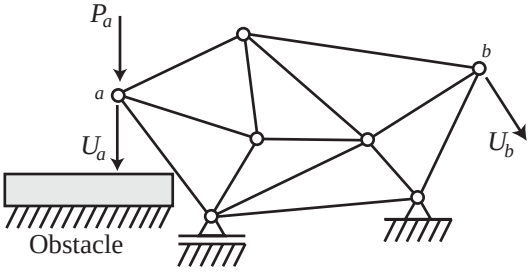

Fig. 26: A plane truss model.

7 Examples of a flexible truss.

In this section, optimization results are presented for a flexible truss allowing large deformation and snapthrough before reaching the final state. It will be shown that snapthrough behavior can be effectively incorporated to obtain a bistable structure that cannot be realized within the range of small deformation. There are only few researches that extensively utilize the effect of large deformation. Bruns *et al.* (6) and Sekimoto and Noguchi (56) presented methods utilizing the effect of snapthrough. However, no bistable mechanism has been generated in their studies.

Consider a plane truss as shown in Fig. 26. Let U_a denote the displacement in the specified direction of node a where a forced displacement is given. A lower-bound $\bar{U}_b$ is assigned for the displacement U_b in the specified direction of node b to ensure the flexibility of the truss. The design requirements for the optimization problem are given as

1. A large deformation is realized within small external force by utilizing the snapthrough behavior, where deformation is controlled by the forced displacement for U_a in the specified direction at node a.
2. The final state is defined such that a displacement U_b in the specified direction at node b reaches the prescribed value $\bar{U}_b$.
3. At the final state, the external load P_a^{f} corresponding to U_a^{f} vanishes, where the superscript $(\ )^{\mathrm{f}}$ indicates a value at the final state.
4. An obstacle is supposed to be placed as shown in Fig. 26 so that node a contacts the obstacle exactly at the final state and the equilibrium state can be stabilized by applying a small force to fix the node to the obstacle.
5. The truss has enough stiffness at the initial state; i.e. the linear responses U_i^0 for some selected displacement components for the unit loads $P_i = 1$, respectively, should be less than the specified value $\bar{U}_i^0$, where the superscript $(\ )^0$ indicates a value corresponding to a unit load.
6. The truss has enough stiffness also at the final state after fixing the node a to the obstacle; i.e. the incremental responses $U_i^{\mathrm{f}0}$ for some selected displacement components for the unit loads $P_i = 1$, respectively, at the final state should be less than the specified value $\bar{U}_i^{\mathrm{f}0}$, where the tangent stiffness is used for computing the displacements.

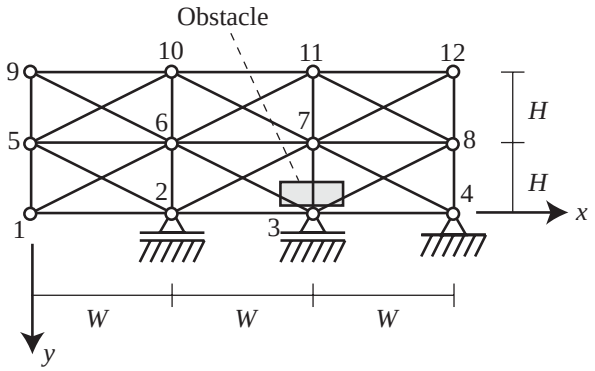

Fig. 27: A 3×2 plane truss.

7. The initial undeformed state can be easily recovered by applying a small external force at node a at the final state.
8. The design variables are the vectors of cross-sectional areas $\mathbf{A} = \{A_i\}$ and nodal locations $\mathbf{X} = \{X_i\}$.
9. The total structural volume $V(\mathbf{A}, \mathbf{X})$ is minimized as the objective function.
   Hence, the optimization problem is formulated as

$$\begin{aligned}
&\text{minimize} && V(\mathbf{A}, \mathbf{X}) && (30)\\
&\text{subject to} && P_a^{\mathrm{f}}(\mathbf{A}, \mathbf{X}) \le 0 && (31)\\
&&& U_i^0(\mathbf{A}, \mathbf{X}) \le \bar{U}_i^0, \quad (i \in I^0) && (32)\\
&&& U_i^{f0}(\mathbf{A}, \mathbf{X}) \le \bar{U}_i^{f0} \quad (i \in I^{\mathrm{f0}}) && (33)\\
&&& A_i^{\mathrm{L}} \le A_i \le A^{\mathrm{U}}, \quad (i = 1, 2, \ldots, n^{\mathrm{A}}) && (34)\\
&&& X_i^{\mathrm{L}} \le X_i \le X_i^{\mathrm{U}}, \quad (i = 1, 2, \ldots, n^{\mathrm{X}}) && (35)
\end{aligned}$$

where X_i^{U} and X_i^{L} are upper and lower bounds for X_i. I^{f0} and I^0 are the lists of displacement components to be considered for evaluating the stiffness. n^{A} and n^{X} are the numbers of variable components in $\mathbf{A}$ and $\mathbf{X}$, respectively. The upper bound A_i^{U} for A_i is sufficiently large, and the lower bound A_i^{L} is a very small value so that the member with $A_i = A_i^{\mathrm{L}}$ after optimization is to be removed.

Consider a 3×2 plane grid truss as shown in Fig. 27. The truss has 29 members and 12 nodes indicated by blank circles including supports. The pairs of intersecting members are not connected with each other. Let $W = 200$ mm, $H = 100$ mm, $E = 200$ GPa. The units of force and length are kN and mm also for this example. The equilibrium path is traced by a displacement increment method, where the norm of unbalanced loads is kept within small value at each increment by carrying out iterative correction using the linear stiffness matrix at the undeformed state. Note that the solution of the equilibrium equation diverges if the full Newton-Raphson method is

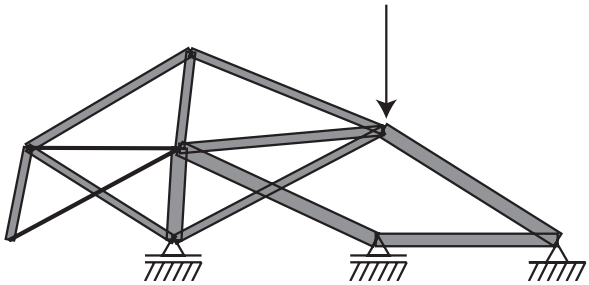

Fig. 28: Optimal cross-sectional areas of the 3×2 plane truss (undeformed configuration).

used. The accuracy of the results has been confirmed by comparing with those by ANSYS Ver. 7.0. Optimization is carried out by IDESIGN Ver. 3.5 (1), where the sequential quadratic programming is used, and the sensitivity coefficients are computed by the finite difference approach. The purpose of the following examples is to present optimal solutions that cannot be achieved if geometrically linear formulation is used, and the computational efficiency is not discussed.

The truss in Fig. 27 represents one of two symmetric parts with respect to the x-axis of equipment composed of bar elements. By applying a vertical load Λp ($p = 100$) in y-direction at node 7, node 1 should move in negative y-direction and be located at the specified position when node 7 reaches an appropriately located obstacle that is illustrated by a gray rectangle in Fig. 27. The node 7 should not move after releasing the load, and should be fixed at the surface of the obstacle by applying small additional load. After reaching this final state, the truss should have enough stiffness, so that small displacement of node 1 should result in a sufficiently large reaction force at node 1.

Let U_{ix} and U_{iy} denote the displacements in x- and y-directions at node i. U_{7y} is taken as the path parameter for the analysis. The final deformed state is defined by $U_{1y} = -500$. Constraints are given as

$$\begin{aligned} U_{7y}^{0} &\leq \bar{U}_{7y}^{0} \\ U_{7x}^{\mathrm{f0}} &\leq \bar{U}_{7x}^{\mathrm{f0}} \\ U_{7y}^{\mathrm{f0}} &\leq \bar{U}_{7y}^{\mathrm{f0}} \end{aligned} \tag{36}$$

where $\bar{U}_{7y}^{0} = 10$, $\bar{U}_{7x}^{f0} = \bar{U}_{7y}^{f0} = 50$.

Let (x_i, y_i) denote the coordinates of node i defined in Fig. 27. The design variables are the cross-sectional area A_i of each member, x_i for $i = 2, 3, 5, 6, 7, 8, 9, 10, 11, 12$, and y_i for $i = 5, 6, 7, 8, 9, 10, 11, 12$. The lower and upper bounds for A_i are 0.01 and 1000, respectively. The location of node i for the initial configuration of the optimization process shown in Fig. 27 is denoted by (x_i^0, y_i^0). The feasible regions for x_i and y_i are given as $x_i^0 - \Delta x \leq x_i \leq x_i^0 + \Delta x$ and $y_i^0 - \Delta y \leq y_i \leq y_i^0 + \Delta y$, respectively, if x_i or y_i is chosen as design variable, where $\Delta x = \Delta y = 20$.

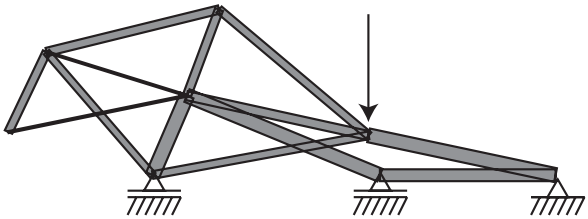

Fig. 29: Optimal cross-sectional areas of the 3×2 plane truss (final configuration).

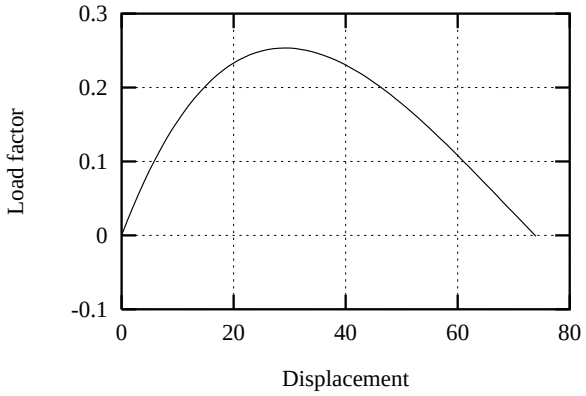

Fig. 30: Relation between U_{7x} and Λ of the optimal truss.

The optimal truss is as shown in Fig. 28, where the width of each member is proportional to its cross-sectional area, and $V = 50.282$. The deformed final configuration is also shown in Fig. 29. The vertical displacement of node 1 reaches 50 at $U_{7y} \simeq 76$. The relation between U_{7y} and Λ is plotted in Fig. 30. If an obstacle is located at the final location of node 7 corresponding to $U_{7y} \simeq 76$, this final configuration is retained by applying a small force, because Λ vanishes at the final state. This way, a bistable structure can be generated by optimization utilizing snapthrough behavior.

8 Concluding remarks.

Difficulties in optimization for geometrically nonlinear buckling behavior have been summarized, and a new optimization results of flexible truss has been presented. The conclusions drawn from this study are summarized as follows:

1. Design sensitivity analysis for regular states can be carried out easily based on the response quantities at the final load level. However, sensitivity coefficients at the critical states cannot be obtained similarly, because the tangent stiffness matrix is singular at the critical point. Furthermore, the sensitivity coefficients may be unbounded at a limit point, or at a degenerate critical point even for a symmetric design modification that corresponds to a minor or second order imperfection.
2. The critical point disappears if the perfect system has a stable symmetric bifurcation point. In this case, the maximum load may be defined in reference to displacements

and stresses of imperfect systems with specified norm of critical imperfection. However, symmetric minor imperfection may be more critical than asymmetric major imperfection.

3. The optimized structure may be extremely sensitive to imperfection due to modal interaction at the coincident critical points if only bifurcation points coincide. However, the imperfection sensitivity of hill-top branching points that have bifurcation points at a limit point are not sensitive to initial imperfection. The difference between the two cases should be clearly noted in discussing the validity of obtaining optimal solutions under constraints on nonlinear buckling loads.
4. A snapthrough behavior can be effectively utilized for obtaining a flexible optimal design that cannot be achieved by a geometrically linear structure. A bistable structure can be effectively generated by optimization.

There is no globally convergent optimization algorithm for large structural systems if geometrical nonlinearity is considered. Since nonlinear path-following analysis itself is computationally costly, heuristic or trial-and-error approach that requires equilibrium analysis many times before reaching the optimal solution should be avoided. Understanding the cause of discontinuity and divergence will be the first step toward a globally convergent algorithm.

Acknowledgement

The author is grateful to Prof. Nishiwaki of Kyoto University for suggesting the problem formulations of the examples of the flexible truss.

References

[1] J.S. Arora and C.H. Tseng. Idesign user's manual, ver. 3.5. Technical report, Optimal Design Laboratory, The University of Iowa, 1987.

[2] K. J. Bathe. *Finite Element Procedures*. Prentice-Hall, 1996.

[3] Z. P. Bažant and Y. Xiang. Postcritical imperfection-sensitive buckling and optimal bracing of large regular frames. *J. Struct. Engng., ASCE*, 123(4):513–522, 1997.

[4] B. Bochenek. Optimization of geometrically nonlinear structures with respect to both buckling and postbuckling constraints. *Eng. Opt.*, 29:401–415, 1997.

[5] B. Bochenek. Problem of structural optimization for post-buckling behavior. *Structural Optimization*, 25:423–435, 2003.

[6] T. E. Bruns, O. Sigmund, and D. A. Tortorelli. Numerical methods for the topology optimization of structures that exhibit snap-through. *Int. J. Num. Meth. Engng.*, 55:1215–1237, 2002.

[7] J. B. Cardoso and J. S. Arora. Variational method for design semsitivity analysis in nonlinear structural mechanics. *AIAA J.*, 26(5):595–603, 1988.

[8] M. A. Crisfield. *Non-linear finite Element Analysis of Solids and Structures*. Wiley, 1991.

[9] H. de Boer and F. van Keulen. Refined semi-analytical design sensitivities. *Int. J. Solids Struct.*, 37:6961–6980, 2000.

[10] F.Fujii, K. Ikeda, H. Noguchi, and S. Okazawa. Modified stiffness iteration to pinpoint multiple bifurcation points. *Comp. Meth. Appl. Mech. Engng.*, 190:2499–2522, 2001.

[11] L. A. Godoy and E. O. Taroco. Design sensitivity of post-buckling states including material constraints. *Comp. Meth. Appl. Mech. Engng.*, 188:665–679, 200.

[12] R. T. Haftka. Semi-analytical static nonlinear structural sensitivity analysis. *AIAA J.*, 31(7):1307–1312, 1993.

[13] S. K. Hall, G. E. Cameron, and D. E. Grierson. Least-weight design of steel frameworks accounting for p-δ effects. *J. Struct. Engng., ASCE*, 115(6):1463–1475, 1988.

[14] E. J. Haug and J. Cea, editors. *Optimization of Distributed Parameter Structures, Vol. 1, 2.* Noordhoff, 1981.

[15] K. D. Hjelmstad and S. Pezeshk. Optimal design of frames to resist buckling under multiple load cases. *J. Struct. Engng., ASCE*, 117(3):915–935, 1991.

[16] G. W. Hunt. Hidden (a)symmetries of elastic and plastic bifurcation. *Appl. Mech. Rev.*, 39(8):1165–1186, 1986.

[17] K. Huseyin. *Nonlinear Theory of Elastic Stability.* Noordhoff, 1975.

[18] K. Ikeda and K. Murota. Critical initial imperfection of structures. *Int. J. Solids Struct.*, 26(8):865–886, 1990.

[19] K. Ikeda, M. Ohsaki, and Y. Kanno. Imperfection sensitivity of hilltop branching points of systems with dihedral group symmetry. *Int. J. Nonlinear Mech., in press*, 2005.

[20] K. Ikeda, K. Oide, and K. Terada. Imperfection sensitive variation of critical loads at hilltop bifurcation point. *Int. J. Eng. Sci.*, 40:743–772, 2002.

[21] M. P. Kamat and P. Ruangsingha. Optimization of space trusses against instability using design sensitivity derivatives. *Eng. Opt.*, 8:177–188, 1985.

[22] Y. Kanno, M. Ohsaki, and N. Katoh. Sequential semidefinite programming for optimization of framed structures under multimodal buckling constraints. *Int. J. Structural Stability and Dynamics*, 1(4):585–602, 2001.

[23] N. S. Khot and M. P. Kamat. Minimum weight design of truss structures with geometric nonlinear behavior. *AIAA J.*, 23:139–144, 1985.

[24] N. S. Khot, V. B. Venkayya, and L. Berke. Optimum structural design with stability constraints. *Int. J. Num. Meth. Engng.*, 10:1097–1114, 1976.

[25] M. Kleiber. *Parameter Sensitivity in Nonlinear Mechanics.* John Wiley & Sons, 1997.

[26] W. T. Koiter. *On the Stability of Elastic Equilibrium.* Ph. D. dissertation, Delft, Holland, 1945. English Translation, NASA, TTF-10833, 1967.

[27] L. Kollár, editor. *Structural Stability in Engineering Practice.* E & FN Spon, 1999.

[28] A. N. Kounadis. Interaction of the joint and of the lateral bracing stiffnesses for the optimum design of unbraced frames. *Acta Mechanica*, 47:247–262, 1983.

[29] M. Kočvara. On the modelling and solving of the truss design problem with global stability constraints. *Structural Optimization*, 23:189–203, 2002.

[30] T. S. Kwon, B. C. Lee, and W. J. Lee. An approximation technique for design sensitivity analysis of the critical load in non-linear structures. *Int. J. Num. Meth. Engng.*, 45:1727–1736, 1999.

[31] L. Léotoing, S. Drapier, and A. Vautrin. Nonlinear interaction of geometrical and material properties in sandwich beam instabilities. *Int. J. Solids Struct.*, 39:3717–3739, 2002.

[32] R. Levy and H. Perng. Optimization for nonlinear stability. *Comp. & Struct*, 30(3):529–535, 1988.

[33] C-C. Lin and I-W Liu. Optimal design based on optimality criterion for frame structures including buckling constraints. *Comp. & Struct*, 31(4):535–544, 1989.

[34] Z. Mróz and R. T. Haftka. Design sensitivity analysis of non-linear structures in regular and critical states. *Int. J. Solids Struct.*, 31(15):2071–2098, 1994.

[35] Z. Mróz and J. Piekarski. Sensitivity analysis and optimal design of non-linear structures. *Int. J. Num. Meth. Engng.*, 42:1231–1262, 1998.

[36] H. Noguchi and T. Hisada. Sensitivity analysis in post-buckling problems of shell structures. *Comp. & Struct*, 47(4):669–710, 1993.

[37] H. Noguchi and T. Hisada. Developement of a sensitivity analysis method for nonlinear buckling load. *JSME Int. J.*, 38(3):311–317, 1995.

[38] M. Ohsaki. Optimization of geometrically nonlinear symmetric systems with coincident critical points. *Int. J. Num. Meth. Engng.*, 48:1345–1357, 2000.

[39] M. Ohsaki. Sensitivity analysis and optimization corresponding to a degenerate critical point. *Int. J. Solids Struct.*, 38:4955–4967, 2001.

[40] M. Ohsaki. Maximum loads of imperfect systems corresponding to stable bifurcation. *Int. J. Solids Struct.*, 39:927–941, 2002.

[41] M. Ohsaki. Sensitivity analysis of an optimized bar-spring model with hill-top branching. *Archive of Applied Mechanics*, 73:241–251, 2003.

[42] M. Ohsaki and T. Nakamura. Optimum design with imperfection sensitivity coefficients for limit point loads. *Structural Optimization*, 8:131–137, 1994.

[43] M. Ohsaki and K. Uetani. Sensitivity analysis of bifurcation load of finite dimensional symmetric systems. *Int. J. Num. Meth. Engng.*, 39:1707–1720, 1996.

[44] M. Ohsaki, K. Uetani, and M. Takeuchi. Optimization of imperfection-sensitive symmetric systems for specified maximum load factor. *Comp. Meth. Appl. Mech. Engng.*, 166:349–362, 1998.

[45] N. Olhoff. Optimal design with respect to structural eigenvalues. In *Proc. 15th Int. IUTAM Congress*, pages 133–149, 1980.

[46] G.V. Palassopoulos. On the optimization of imperfection-sensitive structures with buckling constraints. *Eng. Opt.*, 17:219–227, 1991.

[47] J. S. Park and K. K. Choi. Design sensitivity analysis of critical load factor for nonlinear strutural systems. *Comp. & Struct*, 36(5):823–838, 1990.

[48] J. Pietrzak. An alternative approach to optimization of structures prone to instability. *Structural Optimization*, 11:88–94, 1996.

[49] R. H. Plaut, P. Ruangsilasingha, and M. P. Kamat. Optimization of an asymmetric two-bar truss against instability. *J. Struct. Mech.*, 12(4):465–470, 1984.

[50] W. Prager and J. E. Taylor. Problem of optimal structural design. *J. Appl. Mech.*, pages 102–106, 1968.

[51] R. Reitinger, K.-U. Bletzinger, and E. Ramm. Shape optimization of buckling sensitive structures. *Computing Sys. Engng.*, 5:65–75, 1994.

[52] E. Riks. *Buckling analysis of elastic structures: a computational approach*, volume 34, pages 1–76. Academic Press, 1998.

[53] J. Roorda. On the buckling of symmetric structural systems with first and second order imperfections. *Int. J. Solids Struct.*, 4:1137–1148, 1968.

[54] Y. S. Ryu, M. Harrian, C. C. Wu, and J. S. Arora. Structural design sensitivity analysis of nonlinear response. *Comp. & Struct*, 21(1):245–255, 1985.

[55] M. P. Saka and M. Ulker. Optimum design of geometrically nonlinear space trusses. *Comp. & Struct*, 42(3):289–299, 1991.

[56] T. Sekimoto and H. Noguchi. Homologous topology optimization in large displacement and buckling problems. *JSME Int. J., Series A*, 44:610–615, 2001.

[57] A. P. Seyranian, E. Lund, and N. Olhoff. Multiple eigenvalues in structural optimization problem. *Structural Optimization*, 8:207–227, 1994.

[58] J. Takagi and M. Ohsaki. Design of lateral braces for columns considering critical imperfection of buckling. *Int. J. Structural Stability and Dynamics*, 4(1):69–88, 2004.

[59] J. M. T. Thompson. A general theory for the equilibrium and stability of discrete conservative systems. *ZAMP*, 20:797–846, 1969.

[60] J. M. T. Thompson. *Instabilities and Catastrophes in Science and Engineering*. John Wiley & Sons, 1982.

[61] J. M. T. Thompson and G. W. Hunt. *A General Theory of Elastic Stability*. John Wiley & Sons, 1973.

[62] J. M. T. Thompson and G. W. Hunt. Dangers of structural optimization. *Eng. Opt.*, 1:99–110, 1974.

[63] J. M. T. Thompson and G. W. Hunt. *Elastic Instability Phenomena*. John Wiley & Sons, 1984.

[64] C. A. Vidal and R. B. Haber. Design sensitivity analysis for rate-independent elastoplasticity. *Comp. Meth. Appl. Mech. Engng.*, 107:393–431, 1993.

[65] C. A. Vidal, H.-S. Lee, and R. B. Haber. The consistent tangent operator for design sensitivity analysis of history-dependent response. *Computing Sys. in Engng.*, 2:509–523, 1991.

[66] P. Wriggers and J. C. Simo. A general procedure for the direct computation of turning and bifurcation points. *Int. J. Num. Meth. Engng.*, 30:155–176, 1990.

[67] C. C. Wu and J. S. Arora. Design sensitivity analysis of non-linear buckling load. *Computational Mechanics*, 3:129–140, 1988.